J. Fluid Mech. (1978), *vol.* 84, *part* 3, *pp.* 401–410
Printed in Great Britain

Growth and decay of perturbations at an interface in a stagnation counterflow

By GARY G. ERICKSON AND D. B. OLFE

Department of Applied Mechanics and Engineering Sciences,
University of California, La Jolla

(Received 21 October 1976 and in revised form 3 August 1977)

Integral-transform theory is used to solve the problem of sinusoidal initial perturbations in a planar stagnation counterflow, with extension to the axisymmetric case. The two incompressible fluids are assumed to be inviscid, so that across the initially plane interface the velocity shear is a velocity slip which grows linearly with the distance from the stagnation point. The solution for the interface displacement shows a competition between an amplification produced by the shear instability and a decay produced by the stretching effect of the accelerating unperturbed flow. At early times the interface perturbation grows exponentially with time, but eventually the stretching process reduces the interface displacement to a magnitude comparable to the initial perturbation.

1. Introduction

The classical studies of the linear instability of two incompressible, inviscid, parallel flows with constant velocities were made by Helmholtz (1868), Kelvin (1871) and Rayleigh (1879). Although these studies have been extended to include viscosity, compressibility, magnetic interactions and other real-gas effects, little effort has been made to extend the classical studies to non-parallel flows. For example, in describing a stagnation-counterflow type of situation in the shock layer of an entry probe with 'massive blowing', Compton (1972) was forced to use the classical Kelvin–Helmholz formula for constant parallel flows. Because the stagnation-counterflow geometry occurs in a wide variety of fluid-dynamics problems, detailed study of this flow geometry should be warranted.

2. Equations and boundary conditions

We examine the development of displacement perturbations introduced into an initially plane interface between opposing stagnation flows. A typical cross-section of the counterflow configuration is shown schematically in figure 1. (For illustrative purposes, the sinusoidal perturbation has been greatly magnified.) Surface tension is neglected. Each flow is assumed to be homogeneous, inviscid and incompressible. These assumptions imply irrotationality; thus the velocity field $\mathbf{V}$ in each region can be determined from the gradient of the sum of a time-independent potential $\hat{\phi}$ for the unperturbed flow and a time-dependent potential ϕ for the perturbed flow. The unperturbed flows are given by $\hat{\phi}_j = \frac{1}{2}a_j(x^2-y^2)$, where the subscripts $j = 1$ and 2

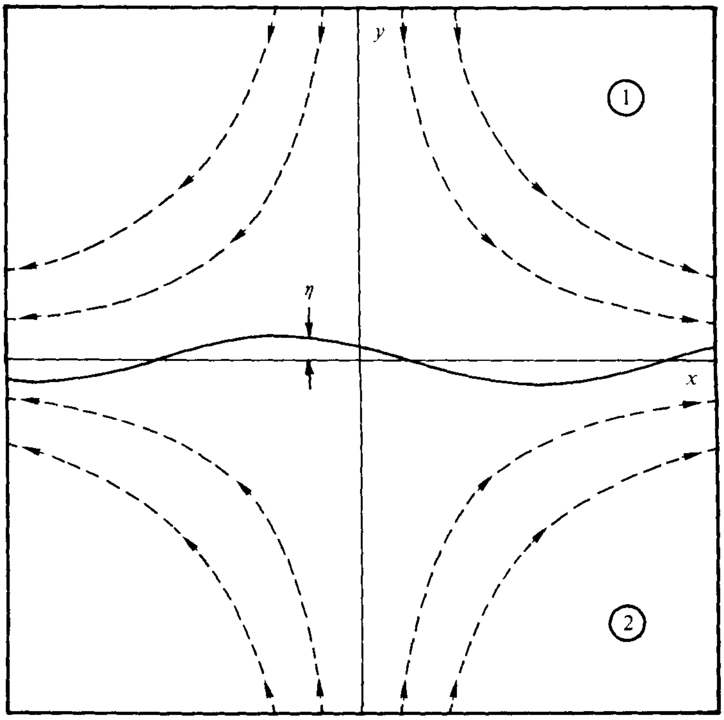

FIGURE 1. A schematic representation of the perturbed interface in a stagnation counterflow.

designate the upper and lower flows, respectively. Application of the incompressible continuity equation shows that the perturbation potential is harmonic in each region, i.e.

$$\nabla^2\phi_j(x, y, t) = 0, \tag{1}$$

with the requirement that $\phi_j(x, y, t) \rightarrow 0$ for $y \rightarrow \pm\infty$.

It should be noted that perturbations in the z direction have been omitted, thereby eliminating consideration of longitudinal vortices induced along the curved streamlines by centrifugal forces. Although such perturbations have been studied and measured near stagnation points on blunt bodies (Kestin & Wood 1970), there apparently exists insufficient work to permit a direct quantitative comparison with the Kelvin–Helmholtz type of shear instability that is addressed in this paper. However, it seems reasonable to expect in many cases that shear instability will be more important near the interface than the centrifugal instability. For example, when the free-stream turbulence is low, it appears that centrifugal instability effects will be unimportant (Schlichting 1971).

Define $\eta(x, t)$ as the interface position relative to the plane $y = 0$. Linearization in accordance with small-amplitude wave theory permits the evaluation of ϕ_j and its derivatives at $y = 0$, rather than at $y = \eta$.

As the interface is approached in each region, the pressure is given by

$$P_j = \bar{P}_j - \rho_j\left[\tfrac{1}{2}a_j^2 x^2 + a_j x\left(\frac{\partial\phi_j}{\partial x}\right) + \left(\frac{\partial\phi_j}{\partial t}\right)\right] \quad \text{at} \quad y = 0, \tag{2}$$

where $\bar{P}_j$ is the stagnation pressure and ρ_j is the density. From the requirement that no pressure discontinuity exists at the unperturbed interface at $y = 0$, we require

$$a_1/a_2 = (\rho_2/\rho_1)^{\frac{1}{2}} \equiv r. \tag{3}$$

After equating the two pressures given by (2) and using (3), the dynamic boundary condition for the interface is

$$\left(\frac{\partial \phi_1}{\partial t}\right) - r^2\left(\frac{\partial \phi_2}{\partial t}\right) + a_1 x\left[\left(\frac{\partial \phi_1}{\partial x}\right) - r\left(\frac{\partial \phi_2}{\partial x}\right)\right] = 0 \quad \text{at} \quad y = 0. \tag{4}$$

The corresponding kinematic boundary conditions are that the normal velocities of the fluids at $y = 0$ must match the rate of change of the interface displacement η. Together with (3), these conditions can be expressed as

$$\left(\frac{\partial \phi_1}{\partial y}\right) = \frac{\partial \eta}{\partial t} + a_1 x \frac{\partial \eta}{\partial x} \quad \text{at} \quad y = 0, \tag{5}$$

$$\left(\frac{\partial \phi_2}{\partial y}\right) = \frac{\partial \eta}{\partial t} + \frac{a_1 x}{r}\frac{\partial \eta}{\partial x} \quad \text{at} \quad y = 0. \tag{6}$$

For initial conditions, we choose

$$\eta(x, 0) = \epsilon \cos(k_0 x + \alpha), \tag{7}$$

$$(\partial \eta/\partial t)_{t=0} = \epsilon[\sigma_1 \cos(k_0 x + \alpha) + \sigma_2 k_0 x \sin(k_0 x + \alpha)], \tag{8}$$

where ϵ is an arbitrarily small amplitude factor, k_0 is an initial perturbation wave-number, α is a phase angle and $\sigma_{1,2}$ are arbitrary constants. The form of the $(\partial \eta/\partial t)_{t=0}$ perturbation given by (8) was chosen so that the $\partial \eta/\partial t$ and the $\partial \eta/\partial x$ terms give similar contributions to the velocity perturbations in (5) and (6). For the purpose of integral-transform evaluation, terms involving η and its derivatives at $x = \pm\infty$ may be set equal to zero. A heuristic way of visualizing this assumption is to consider the perturbations to be truncated at large finite positive and negative values of x, and then to let the truncation distances approach $\pm\infty$. As a verification of the procedure, the final solution will be shown to satisfy the governing equations (1)–(8).

A further indication of the validity of the procedure is given in appendix A, where the stagnation counterflow is assumed to be embedded in a velocity profile which takes on constant values at large x.

3. The solution for the interface displacement

Development of a partial differential equation for the interface displacement

A systematic approach to this initial-value problem is to apply integral-transform theory. We begin by applying a Fourier transform with respect to x. The convention in the notation for this Fourier transform operator and its inverse $\mathscr{F}^{-1}$ is

$$\left.\begin{aligned} \bar{f}(k) \equiv \mathscr{F}\{f\} &\equiv \int_{-\infty}^{\infty} f(x)\, e^{-ikx}\, dx, \\ f(x) = \mathscr{F}^{-1}\{\bar{f}\} &= \frac{1}{2\pi}\int_{-\infty}^{\infty} \bar{f}(k)\, e^{ikx}\, dx. \end{aligned}\right\} \tag{9}$$

The following transformations are considered:

$$\Phi_j(k,y,t) \equiv \mathscr{F}\phi_j, \quad Y(k,t) \equiv \mathscr{F}\eta. \tag{10}$$

Transformation of (1) yields

$$\partial^2\Phi_j/\partial y^2 - k^2\Phi_j = 0, \quad \Phi_j = F_j(k,t)\,e^{\mp|k|y}, \tag{11\,a,b}$$

where in (11 b) the minus sign is chosen in the exponent for $y > 0$ and the plus sign for $y < 0$.

The application of (10) and (11) to the boundary conditions (4), (5) and (6) leads to the following equations in the Fourier transform space:

$$F_1 = \frac{1}{|k|}\left[a_1\left(1 + k\frac{\partial}{\partial k}\right) - \frac{\partial}{\partial t}\right] Y, \tag{12}$$

$$F_2 = -\frac{1}{r|k|}\left[a_1\left(1 + k\frac{\partial}{\partial k}\right) - r\frac{\partial}{\partial t}\right] Y, \tag{13}$$

$$\left[\frac{\partial}{\partial t} - a_1\left(1 + k\frac{\partial}{\partial k}\right)\right] F_1 - \left[r\frac{\partial}{\partial t} - a_1\left(1 + k\frac{\partial}{\partial k}\right)\right](rF_2) = 0, \tag{14}$$

where the operator $-(1 + k\,\partial/\partial k)\,Y$ represents $\mathscr{F}\{x\,\partial\eta/\partial x\}$. Following the elimination of F_1 and F_2 among (12)–(14), a second-order partial differential equation for Y is obtained. After taking the inverse Fourier transform of this equation for Y, the following elliptic, second-order, partial differential equation for the interface displacement is found:

$$2a_1^2 x^2 \frac{\partial^2\eta}{\partial x^2} + 4a_1^2 x \frac{\partial\eta}{\partial x} + (1+r)\,a_1\left[\frac{\partial\eta}{\partial t} + 2x\frac{\partial^2\eta}{\partial x\,\partial t}\right] + (1+r^2)\frac{\partial^2\eta}{\partial t^2} = 0. \tag{15}$$

Equation (15) represents a combination of the two solutions to Laplace's equation (1), the two kinematic boundary conditions (5) and (6) and the dynamic boundary condition (4).

The solution to the partial differential equation for the interface displacement

An algebraic expression for η in transform space may be derived from (15) by taking a Laplace transform with respect to t and a Mellin transform with respect to x. The conventions in the notation for the Laplace and Mellin transforms, designated by the operators $\mathscr{L}$ and $\mathscr{M}$, are

$$\left.\begin{aligned} \tilde{g}(p) &\equiv \mathscr{L}\{g(t)\} \equiv \int_0^\infty g(t)\,e^{-pt}\,dt, \\ g(t) &= \mathscr{L}^{-1}\{\tilde{g}(p)\} = \frac{1}{2\pi i}\int_{c-i\infty}^{c+i\infty} \tilde{g}(p)\,e^{pt}\,dp \end{aligned}\right\} \tag{16}$$

and

$$\left.\begin{aligned} \tilde{h}(s) &\equiv \mathscr{M}\{h(x)\} \equiv \int_0^\infty h(x)\,x^{s-1}\,dx, \\ h(x) &= \mathscr{M}^{-1}\{\tilde{h}(s)\} = \frac{1}{2\pi i}\int_{N-i\infty}^{N+i\infty} \tilde{h}(s)\,x^{-s}\,ds. \end{aligned}\right\} \tag{17}$$

As is customary, $\tilde{g}(p)$ is required to have no singularities in the region $\mathrm{Re}\,p \geqslant c$, whereas $\tilde{h}(s)$ is to be absolutely convergent in an infinite strip parallel to (and perhaps including) the imaginary s axis.

The application of the Laplace transform with respect to t to (15) eliminates the derivatives of t, and also incorporates the initial conditions (7) and (8) into the solution. The choice of a Mellin transform with respect to x is natural because it eliminates the x derivatives according to the relationship

$$\mathscr{M}\{x^n\,\partial^n f(x)/\partial x^n\} = (-1)^n s(s+1)\ldots(s+n-1)\,\Gamma(s),$$

where $\Gamma(s)$ is the gamma function. It should be noted that the Mellin transformation brings in no values or derivatives of $f(x)$ at $x = 0$. This fact is of special significance because it justifies the use of the integration limits $(0, \infty)$ in (17), rather than choosing another transform which has integration limits $(-\infty, \infty)$. Mathematically, the Mellin transform implies that two different solutions for $x < 0$ and $x > 0$ are possible (provided the pressure and x velocity components are continuous across $x = 0$). Physically, this means that the left and right regions of the stagnation counterflow are decoupled from each other. Such a decoupling could be heuristically anticipated from (15) because the $x^n\,\partial^n\eta/\partial x^n$ terms originate from products of the unperturbed flow velocities and perturbation quantities. Hence the advective flow away from the stagnation point prevents communication across $x = 0$. For the remainder of this paper, x will be implicitly restricted to $x \geqslant 0$. However, the results are applicable for $-\infty < x < \infty$ since the same formulae are valid for negative x. Define the non-dimensional variables

$$\xi \equiv k_0 x, \quad m \equiv (1+r)/(1+r^2), \quad \tau \equiv m a_1 t \tag{18}$$

and set

$$Z(\xi,p) \equiv \mathscr{L}\{\eta(\xi,t)\}, \quad W(\xi,s) \equiv \mathscr{M}\{Z(\xi,p)\}. \tag{19}$$

Then, taking the Laplace transform of (15), we find that

$$\begin{aligned} 2a_1^2\xi^2\frac{\partial^2 Z}{\partial\xi^2} &+ 2a_1[2a_1+(1+r)p]\,\xi\frac{\partial Z}{\partial\xi} + p[(1+r)a_1+(1+r^2)p]\,Z \\ &= \left\{(1+r^2)p+(1+r)a_1\left[1+2\xi\frac{\partial}{\partial\xi}\right]\right\}\eta\bigg|_{t=0} + (1+r^2)\frac{\partial\eta}{\partial t}\bigg|_{t=0}. \end{aligned} \tag{20}$$

After introducing the initial conditions and applying the Mellin transform, the following algebraic solution is obtained:

$$\begin{aligned} W(s,p) &= \epsilon\{p+\sigma_1+ma_1+(\sigma_2-2ma_1)s\}\,\Gamma(s)\cos(\tfrac{1}{2}\pi s+\alpha) \\ &\quad\times\{p^2+ma_1(1-2s)p+[2a_1^2 s(s-1)/(1+r^2)]\}^{-1}, \end{aligned} \tag{21}$$

with $0 < \operatorname{Re} s < 1$. In (21) the products $\Gamma(s)\cos(\frac{1}{2}\pi s+\alpha)$ and $s\Gamma(s)\cos(\frac{1}{2}\pi s+\alpha)$ originate from $\mathscr{M}\{\cos(\xi+\alpha)\}$ and $\mathscr{M}\{\xi\sin(\xi+\alpha)\}$, respectively.

The solution for the interface displacement is just $\mathscr{M}^{-1}\mathscr{L}^{-1}\{W(s,p)\}$, or

$$\eta(\xi,\tau) = -\frac{1}{4\pi^2}\int_{N-i\infty}^{N+i\infty}\int_{c-i\infty}^{c+i\infty}\exp(p\tau/ma_1)\,\xi^{-s}W(s,p)\,dp\,ds. \tag{22}$$

Inspection of (21) shows that $W(s,p)$ has two first-order poles in the p plane and is well behaved otherwise. Thus the inverse Laplace transform may be evaluated by residue theory to give

$$\eta(\xi,\tau) = \frac{\epsilon}{2\pi i}\int_{N-i\infty}^{N+i\infty}\Gamma(s)\cos\left(\frac{\pi s}{2}+\alpha\right)\xi^{-s}G(s,\tau)\,ds, \quad 0 < N < 1, \tag{23}$$

where

$$\left.\begin{aligned} G(s,\tau) &= e^{(s-\frac{1}{2})\tau}[\cosh\{\Omega(s)\tau\}+A(s)\,\Omega^{-1}(s)\sinh\{\Omega(s)\tau\}], \\ A(s) &\equiv \tfrac{1}{2}+\sigma_1/ma_1+(\sigma_2/ma_1-1)\,s, \\ \Omega(s) &\equiv \tfrac{1}{2}[1+4\theta^2(s-s^2)]^{\frac{1}{2}}, \quad \theta \equiv (1-r)/(1+r). \end{aligned}\right\} \tag{24}$$

Although $\Omega(s)$ is multi-valued in the s plane, examination shows that $G(s, \tau)$ is single-valued. To aid in the evaluation of (23), we note that the gamma function $\Gamma(s)$ may be analytically continued into the negative half-plane. Along the negative real axis $\Gamma(s)$ has an infinite number of poles at integer values of s. In particular, near these poles the representation for $\Gamma(s)$ reduces to (see, for example, Lebedev 1972, p. 3)

$$\Gamma(s) = (-1)^l/l!(s+l) + \text{a regular part}, \quad l = 0, 1, 2, \ldots. \tag{25}$$

Therefore we evaluate the inverse Mellin transform by connecting the ends of the infinite line segment with an infinite semicircular contour closed to the left. Evaluation of the residues gives the following solution for the interface displacement:

$$\eta(\xi, \tau) = \epsilon \sum_{l=0}^{\infty} \frac{(-\xi)^l}{l!} \cos\left(-\frac{\pi l}{2} + \alpha\right) G(-l, \tau). \tag{26}$$

It is easily verified that (26) satisfies the prescribed initial conditions (7) and (8), and also the governing equation (15). In appendix B, we derive expressions for the perturbation velocity potentials, and verify that the interface displacement (26) and the velocity potentials satisfy boundary conditions (4)–(6).

4. Asymptotic limits of the infinite series solution for the interface displacement

Introduction

For convenience, let us present (26) in a more explicit form:

$$\eta(\xi, \tau) = \epsilon e^{-\frac{1}{2}\tau} \sum_{l=0}^{\infty} \frac{(-\xi e^{-\tau})^l}{l!} \cos\left(-\frac{\pi l}{2} + \alpha\right) \left\{\cosh\{\tfrac{1}{2}\tau[1 - 4\theta^2(l + l^2)]^{\frac{1}{2}}\} + \frac{[\frac{1}{2} + \sigma_1/ma_1 + (1 - \sigma_2/ma_1)\, l] \sinh\{\frac{1}{2}\tau[1 - 4\theta^2(l + l^2)]^{\frac{1}{2}}\}}{\frac{1}{2}[1 - 4\theta^2(l + l^2)]^{\frac{1}{2}}}\right\}. \tag{27}$$

We note that (27) is appropriately invariant if the stagnation counterflow is inverted.

The factor $\xi e^{-\tau}$ appearing in (27) arises because of the stretching of the initial perturbation wavelength by the accelerating unperturbed shear flow. This behaviour is easily demonstrated by considering the mean unperturbed fluid velocity

$$\overline{U} = (\rho_1 U_1 + \rho_2 U_2)/(\rho_1 + \rho_2) = ma_1 x. \tag{28a, b}$$

By equating the wavelength stretching rate $d\lambda/dt$ to $\overline{U}(x+\lambda) - \overline{U}(x)$ and integrating, it is found that the wavelength increases as $\lambda = \lambda_0 e^{\tau}$. Therefore

$$\xi e^{-\tau} = 2\pi x/(\lambda_0 e^{\tau}) = 2\pi x/\lambda$$

represents the x position non-dimensionalized by the stretched wavelength.

A qualitative understanding of the growth and eventual decay of the displacement perturbations can be gained by considering an upper bound for the right-hand side of (27):

$$\begin{aligned} \eta(\xi, \tau) &< \epsilon[1 + \theta^{-1} + (ma_1)^{-1}(|\sigma_1| + |\sigma_2|\theta^{-1})] \sum_{l=0}^{\infty} \frac{(\xi e^{-\tau})^l}{l!} \\ &= \epsilon[1 + \theta^{-1} + (ma_1)^{-1}(|\sigma_1| + |\sigma_2|\theta^{-1})] \exp(\xi e^{-\tau}). \end{aligned} \tag{29}$$

Hence, at intermediate times $\tau = O(1)$, the interface displacement may attain a maximum value proportional to ϵe^{ξ}, but, at large times when $\tau \gg 1$, the displacement will decay to $O(\epsilon)$. Note that the e^{ξ} factor arises from the fact that the x components of the unperturbed velocities grow linearly with ξ for the stagnation flows. For the more general unperturbed velocity profiles considered in appendix A, the velocities approach constant values at large ξ, and the perturbed interface would cease to grow with ξ at sufficiently large ξ.

For $\tau = 0$, (27) and its derivative with respect to τ can be summed directly to give the initial conditions (7) and (8).

The limit $\xi e^{-\tau} \gg 1$

The limit $\xi e^{-\tau} \gg 1$ of (27) illustrates the growth of a disturbance of small wavelength at early times. In this limit, the large-l terms make the greatest contribution to the summation. Consequently, by approximating each term in (27) by its large-l limit, the summation may be carried out to give

$$\begin{aligned}\eta(\xi,\tau) \simeq \epsilon e^{-\frac{1}{2}\tau}\Bigg\{&\left[\cos\left(\frac{\theta\tau}{2}\right)+\theta^{-1}\left(1-\frac{\sigma_2}{ma_1}\right)\sin\left(\frac{\theta\tau}{2}\right)\right]\\ &\times\cos\left[\xi e^{-\tau}\cos(\theta\tau)+\alpha\right]\cosh\left[\xi e^{-\tau}\sin(\theta\tau)\right]\\ &+\left[\sin\left(\frac{\theta\tau}{2}\right)-\theta^{-1}\left(1-\frac{\sigma_2}{ma_1}\right)\cos\left(\frac{\theta\tau}{2}\right)\right]\\ &\times\sin\left[\xi e^{-\tau}\cos(\theta\tau)+\alpha\right]\sinh\left[\xi e^{-\tau}\sin(\theta\tau)\right]\Bigg\}.\end{aligned} \tag{30}$$

Equation (30) shows that for $\xi e^{-\tau} \gg 1$ the displacement has the upper bound

$$\eta(\xi,\tau) < \epsilon(1+\theta^{-1}|1-\sigma_2/ma_1|)\exp\left[\xi e^{-\tau}-\tfrac{1}{2}\tau\right].$$

The fact that this maximum amplitude is proportional to $\epsilon\exp(\xi e^{-\tau})$ agrees with the qualitative discussion in the introduction to this section. We note that the sinusoidal variation with distance involves the non-dimensional stretched co-ordinate $\xi e^{-\tau}$ multiplied by a sinusoidal function of time.

When $\tau \ll 1$, a fluid particle will have travelled only a small relative distance from its initial position. Therefore the fluid particle will experience a nearly constant unperturbed velocity for $\tau \ll 1$, and the stagnation-counterflow result should reduce to the classical result for perturbations along the interface between two fluids having constant unperturbed velocities. For $\tau \ll 1$ and $\xi\tau = O(1)$, (30) reduces to

$$\eta(\xi,\tau) = \epsilon\left\{\cos\left[\xi(1-\tau)+\alpha\right]\cosh\theta\xi\tau+\theta^{-1}\left(\frac{\sigma_2}{ma_1}-1\right)\sin\left[\xi(1-\tau)+\alpha\right]\sinh\theta\xi\tau\right\}. \tag{31}$$

For comparison, the following is the classical perturbation solution for the interface displacement between two fluids having constant unperturbed velocities (see Rayleigh 1879):

$$\eta(x,t) = B\exp\{[k_0(\rho_1\rho_2)^{\frac{1}{2}}|U_2-U_1|\,t/(\rho_1+\rho_2)]-ik_0[x-\overline{U}t]\}, \tag{32}$$

where B is a constant and $\overline{U}$ is given by (28*a*), with U_1 and U_2 the constant unperturbed velocities. In (31) and (32) the exponential and sinusoidal dependences are equivalent, since for the stagnation counterflow $k_0(\rho_1\rho_2)^{\frac{1}{2}}|U_2-U_1|\,t/(\rho_1+\rho_2) = \theta\xi\tau$ and

$$k_0(x-\overline{U}t) = \xi(1-\tau).$$

Equations (31) and (32) would be identical if the solution (32) were derived for the same initial conditions as (31).

The limit $\xi e^{-\tau} \ll 1$

The limit $\xi e^{-\tau} \ll 1$ corresponds to the situation in which the point x lies near the beginning of the first (stretched) disturbance wavelength. Even when $\xi \gg 1$, the factor $\xi e^{-\tau}$ becomes small when τ is sufficiently large.

For $\xi e^{-\tau} \ll 1$, $\eta(\xi,\tau)$ can be approximated by the leading terms in (27), of which the first two are

$$\eta(\xi,\tau) \simeq \epsilon\cos\alpha\left[\left(1+\frac{\sigma_1}{ma_1}\right)-\frac{\sigma_1}{ma_1}e^{-\tau}\right]-\epsilon\xi\sin\alpha\, e^{-\frac{3}{2}\tau}\left\{\cosh\left[\tfrac{1}{2}\tau(1-8\theta^2)^{\frac{1}{2}}\right]\right.$$
$$\left.+\left[3+2\left(\frac{\sigma_1-\sigma_2}{ma_1}\right)\right](1-8\theta^2)^{-\frac{1}{2}}\sinh\left[\tfrac{1}{2}\tau(1-8\theta^2)^{\frac{1}{2}}\right]\right\}. \quad (33)$$

Thus at $\xi = 0$ the perturbation displacement varies from the initial value of $\epsilon\cos\alpha$ to the value $\epsilon[1+(\sigma_1/ma_1)]\cos\alpha$ as $\tau\to\infty$ (the latter displacement value also occurs at finite ξ when $\xi e^{-\tau}\to 0$).

The limit $r = 1$

The limit $r = 1$ occurs when both stagnation flows have the same density and the same unperturbed velocity. In this case $\theta = 0$, and (27) can be summed to yield

$$\eta(\xi,\tau) = \epsilon\left\{\left[1+\frac{\sigma_1}{a_1}(1-e^{-\tau})\right]\cos(\xi e^{-\tau}+\alpha)+\left(\frac{\sigma_2}{a_1}-1\right)(1-e^{-\tau})(\xi e^{-\tau})\sin(\xi e^{-\tau}+\alpha)\right\}. \quad (34)$$

For small τ, (34) shows that the displacement grows linearly with τ. Equation (34) for small τ and $\xi\tau = O(1)$ corresponds to the famous 'flapping sail' limit of classical theory (see Rayleigh 1879). The reason for the linear growth in time is that the horizontal perturbation velocities, as can be seen in (B 5), have opposite signs across the interface, thereby creating a shear instability.

For large τ, the displacement perturbation (34) approaches a constant value $O(\epsilon)$.

5. The axisymmetric case

Planar stagnation counterflows may be superposed to yield an axisymmetric stagnation counterflow. Consider a planar solution in which the x axis makes an angle $\tilde{\theta}$ with respect to a fixed direction given by the co-ordinate $\tilde{r}$, where $x = \tilde{r}\cos\tilde{\theta}$. Then a proper summation over planar solutions is achieved by dividing by 2π and integrating over $\tilde{\theta}$ from 0 to 2π, while keeping $\tilde{r}$ constant. Such an integration transforms the unperturbed planar potential $\tilde{\phi}_j(x,y)$ into the axisymmetric potential $\tilde{\phi}_j(\tilde{r},y) = \frac{1}{4}a_j(\tilde{r}^2-2y^2)$.

A similar integration over $\tilde{\theta}$ may be carried out for the perturbed interface displacement. It is appropriate to assume $\alpha = 0$ because antisymmetric disturbances will cancel out in the superposition of planar solutions. The resulting interface displacement for the axisymmetric case is

$$\eta(R,\tau) = \frac{\epsilon}{\pi^{\frac{1}{2}}}\sum_{n=0}^{\infty}\frac{(-R^2)^n}{(2n)!}\frac{\Gamma(n+\frac{1}{2})}{\Gamma(n+1)}G(-2n,\tau), \quad (35)$$

where $R \equiv k_0\tilde{r}$. The ratio of gamma functions may be expressed as

$$\Gamma(n+\tfrac{1}{2})/\Gamma(n+1) = [1.3.5\ldots(2n-1)]\,\pi^{\frac{1}{2}}/[2.4.6\ldots 2n].$$

The solution (35) corresponds to the initial conditions $\eta = \epsilon J_0(R)$ and

$$\partial\eta/\partial t = \epsilon[\sigma_1 J_0(R) + \sigma_2 R J_1(R)] \quad \text{at} \quad t = 0.$$

In view of the similarities between (26) and (35), it is concluded that perturbations in the axisymmetric case behave in the same manner as the planar perturbations discussed in the preceding section.

Appendix A. An example of an embedded stagnation counterflow

In order to study further the large-x behaviour of a stagnation counterflow, we consider more realistic velocity profiles which approach constant values at large x; i.e. the x components of the unperturbed velocities for $x > 0$ are assumed to be given by

$$U_j(x, 0) = a_j x/(1+bx), \tag{A 1}$$

where the a_j are related by (3) and b is a positive constant. With the velocity profile (A 1) equations (4)–(6) retain the same form, but with $a_1 x$ replaced by $a_1 x/(1+bx)$.

After multiplying by $1+bx$, the Fourier transforms of the new equations may be taken to yield equations similar to (12)–(14), but with the operator $\partial/\partial t$ replaced by $[1+ib\,\partial/\partial k]\,\partial/\partial t$ and the F_j on the left-hand sides of (12) and (13) replaced by

$$[1+(ib/k)+ib\,\partial/\partial k]\,F_j.$$

After much algebraic manipulation the resulting equations may be combined to yield a single differential equation for Y, which involves third-order derivatives in k. The inverse Fourier transform then yields the following differential equation:

$$\begin{aligned}\left[2a_1^2x^2\frac{\partial^2\eta}{\partial x^2}+4a_1^2x\frac{\partial\eta}{\partial x}+2a_1(1+r)\,x\frac{\partial^2\eta}{\partial x\,\partial t}+a_1(1+r)\frac{\partial\eta}{\partial t}+(1+r^2)\frac{\partial^2\eta}{\partial t^2}\right]&\\ +(bx)^3\left[2\left(\frac{a_1}{b}\right)^2\frac{\partial^2\eta}{\partial x^2}+2\left(\frac{a_1}{b}\right)(1+r)\frac{\partial^2\eta}{\partial x\,\partial t}+(1+r^2)\frac{\partial^2\eta}{\partial t^2}\right]&\\ +a_1(bx)\,(1+r)\left(\frac{\partial\eta}{\partial t}+4x\frac{\partial^2\eta}{\partial x\,\partial t}\right)+3(bx)\,(1+bx)\,(1+r^2)\frac{\partial^2\eta}{\partial t^2}=0.&\end{aligned} \tag{A 2}$$

In the limit $bx \to 0$ equation (A 2) reduces to the first bracketed term, which is identical to the equation (15) for the stagnation-counterflow problem. Thus (15) may be derived as the small bx expansion for the problem having the unperturbed velocity (A 1). This derivation avoids the consideration of unbounded velocities as $x \to \pm\infty$. It is noted that for $bx \gg 1$ the second bracketed term in (A 2) becomes dominant, yielding (for periodic initial conditions) the appropriate Kelvin–Helmholtz solution of the form of (32) for the constant unperturbed velocities $U_1 \to a_1/b$ and $U_2 \to a_2/b$.

Appendix B. The perturbation velocity potentials

We can construct the appropriate ϕ_j from the η solution (26) by means of the kinematic boundary conditions (5) and (6), Laplace's equation (1) and the conditions at $y = \pm\infty$. An integral form for the interface displacement is

$$\left.\begin{aligned}\eta(\xi,\tau) &= \epsilon\int_0^\infty F(w,\tau)\cos(\xi w+\alpha)\,dw,\\ \text{where}\qquad F(w,\tau) &\equiv \mathscr{M}^{-1}[G(1-s,\tau)].\end{aligned}\right\} \tag{B 1}$$

Equation (B 1) may be verified by comparing its Mellin transform with the Mellin transform of (23).

Since we have non-dimensionalized x to ξ and t to τ, for consistency we define $\zeta \equiv k_0 y$. Then by substituting (B 1) into (5) and (6), we determine $\partial\phi_j/\partial\zeta$ at $\zeta = 0$. In order to extend the $\partial\phi_j/\partial\zeta$ expression to finite values of ζ, solutions to Laplace's equation are constructed by appropriately including $\exp(-w\zeta \operatorname{sgn}\zeta)$ and

$$\zeta \operatorname{sgn}\zeta \exp(-w\zeta \operatorname{sgn}\zeta)$$

in the integrand. After integration with respect to ζ the following result is obtained:

$$\left.\begin{aligned}\phi_j(\xi,\zeta,\tau) = \frac{a_1\epsilon(-1)^j}{k_0}\int_0^\infty \exp(-w\zeta\operatorname{sgn}\zeta)\left\{\left(\gamma - m\frac{\partial}{\partial\tau}\right)w^{-1}F(w,\tau)\cos(\xi w+\alpha)\right.\\ \left.+\gamma F(w,\tau)\left[\xi\sin(\xi w+\alpha)+\zeta\operatorname{sgn}\zeta\cos(\xi w+\alpha)\right]\right\}dw,\\ \text{where} \qquad \gamma\equiv 1 \quad \text{in} \quad \phi_1, \quad \gamma \equiv 1/r \quad \text{in} \quad \phi_2.\end{aligned}\right\} \tag{B 2}$$

The dynamic boundary condition given by (4) requires x and t derivatives of the velocity potential only at $\zeta = 0$. Accordingly, we set $\zeta = 0$ in (B 2) and evaluate the integral by a change of variable. The latter is introduced formally by applying a Mellin transform, interchanging the order of integration and then taking the inverse Mellin transform. Equation (B 2) becomes

$$\phi_j(\xi,0,\tau) = \frac{(-1)^j a_1\epsilon}{k_0\, 2\pi i}\int_{N-i\infty}^{N+i\infty}\Gamma(s)\,\xi^{-s}\cos\left(\frac{\pi s}{2}+\alpha\right)\left[(1+s)\gamma - m\frac{\partial}{\partial\tau}\right]G(1+s,\tau)\,ds, \tag{B 3}$$

where $0 < N < 1$. Equation (B 3) is evaluated by the same procedure as that used for (23), giving

$$\phi_j(\xi,0,\tau) = \frac{(-1)^j a_1\epsilon}{k_0}\sum_{l=0}^{\infty}\frac{(-\xi)^l}{l!}\cos\left(-\frac{\pi l}{2}+\alpha\right)\left[(1-l)\gamma - m\frac{\partial}{\partial\tau}\right]G(1-l,\tau). \tag{B 4}$$

The horizontal perturbation velocities at the interface are

$$\left.\frac{\partial\phi_j}{\partial\xi}\right|_{\zeta=0} = \frac{(-1)^j a_1\epsilon}{k_0}\left[m\frac{\partial}{\partial\tau}+\gamma\xi\frac{\partial}{\partial\xi}\right]\sum_{l=0}^{\infty}\frac{(-\xi)^l}{l!}\sin\left(-\frac{\pi l}{2}+\alpha\right)G(-l,\tau). \tag{B 5}$$

The following vertical perturbation velocities at the interface are found by computing $[\partial\phi_j/\partial\zeta]_{\zeta=0}$ from (B 2) and then following a procedure similar to that used in deriving (B 4), or by substituting (26) into (5) and (6):

$$\left.\frac{\partial\phi_j}{\partial\zeta}\right|_{\zeta=0} = \frac{a_1\epsilon}{k_0}\left[m\frac{\partial}{\partial\tau}+\gamma\xi\frac{\partial}{\partial\xi}\right]\sum_{l=0}^{\infty}\frac{(-\xi)^l}{l!}\cos\left(-\frac{\pi l}{2}+\alpha\right)G(-l,\tau). \tag{B 6}$$

For a verification of the solution given by (26), (B 4), (B 5) and (B 6), direct substitution shows that the boundary conditions (4)–(6) are satisfied. Furthermore, the ϕ_j solution (B 2) satisfies Laplace's equation (1).

REFERENCES

Compton, D. L. 1972 *J. Spacecraft* **9**, 717.

Helmholtz, H. 1868 *Phil. Mag.* **36**, 337.

Kelvin, Lord 1871 *Phil. Mag.* **42**, 368.

Kestin, J. & Wood, R. F. 1970 *J. Fluid Mech.* **44**, 461.

Lebedev, N. N. 1972 *Special Functions and Their Applications* (English trans.). Dover.

Rayleigh, Lord 1879 *Proc. Lond. Math. Soc.* **10**, 4.

Schlichting, H. 1971 *J. Appl. Mech.* **38**, 289.